An Image Segmentation Approach for the Detection of Small-scale Magnetic Anomalies

Peggy Gödickmeier[1], Sascha Weit[1], Ralph-Uwe Börner[1], and Klaus Spitzer[1]

[1] *Institute of Geophysics and Geoinformatics*

1 Motivation

Hundreds of thousands of unexploded ordnance (UXO) are still remaining in the subsurface worldwide and pose a high potential hazard. Thus, the urgent need to ensure a safe recovery of such objects requires an improved strategy for analyzing field data acquired by magnetic survey methods. To achieve more accurate localization of UXO, we aim to apply a deep learning framework to recognize their specific magnetic anomaly pattern at the Earth's surface. Using an image segmentation approach, the model is trained to separate a potential target signal from different background fields. Here, we present the generation and processing of training data, the applied network architecture, and preliminary results to prove the concept.

2 Numerical Simulation and Data Engineering

Applying a deep learning framework to correctly interpret magnetic data requires a vast amount of training samples. Due to a lack of real survey data, our segmentation approach is based on synthetic data. The simulation and preparation of adequate training scenarios has been performed using Matlab, and is based on the simulation routine described in Gödickmeier (2020).
Initially, various datasets with 10000 samples were generated randomly. Taking into account the ambiguity and complexity of magnetic field data, every map has been compiled using a certain number of individual simulated field anomalies with different spatial location properties. For this purpose, the simple model of a homogeneously magnetized sphere was assumed as an elementary unit, representing a possible target object. According to Blakely (1996), the magnetic anomaly of a single spherical object was calculated in terms of the magnetic flux density $\mathbf{B}(P)$ at an observation point P outside the sphere. $\mathbf{B}$ is a function of the distance r between the spherical center and P, the dipole moment m, and the relative magnetic permeability μ_0 and reads:

$$\mathbf{B}(P) = \frac{\mu_0 m}{4\pi r^3}\,[3(\hat{\mathbf{m}}\cdot\hat{\mathbf{r}})\hat{\mathbf{r}} - \hat{\mathbf{m}}] \qquad \text{with} \qquad m \;=\; V\cdot M \;=\; \frac{4\pi}{3}a^3\cdot M. \tag{1}$$

$\hat{\mathbf{m}}$ and $\hat{\mathbf{r}}$ are unit vectors in the direction of the dipole axis and the location vector, respectively. The dipole moment of the sphere can be derived from a dipole located in the center of the sphere, where V describes its volume, a its radius, and M the magnetization. Modifying the spatial properties of the simulated objects, such as depth $z = [0, 15]\,\mathrm{m}$ and dipole orientation $(\phi, \theta, \psi) \in \mathbb{R}^3 = [0, 360]^\circ$ in terms of the Euler angles, leads to a complex

measurement scenario. A variation of the dipole orientation has been applied to imprint remanence on the otherwise only induced simulated magnetization. Using predetermined step sizes of $\Delta x = \Delta y = 0.5\,\mathrm{m}$ for observation points (x-direction) and profile spacing (y-direction) over a computational domain of (x, y) $\in \Omega = [\text{-}100,\ 100]\,\mathrm{m}$, a spatially highly resolved, square field of 4 ha is produced (see Fig. 1 left). Depending on the geomagnetic latitude, which is kept constant for all case studies, an exemplary magnetic map representing the assumed investigation area is obtained. In our study, the represented magnetic situation corresponds to the one in Freiberg with a total magnetic intensity (TMI) of about 49400 nT, an inclination of approx. 67 °, and a declination of approx. 4 °. It turns out that the network has to be re-trained for different geomagnetic locations which limits the transferability of this method.

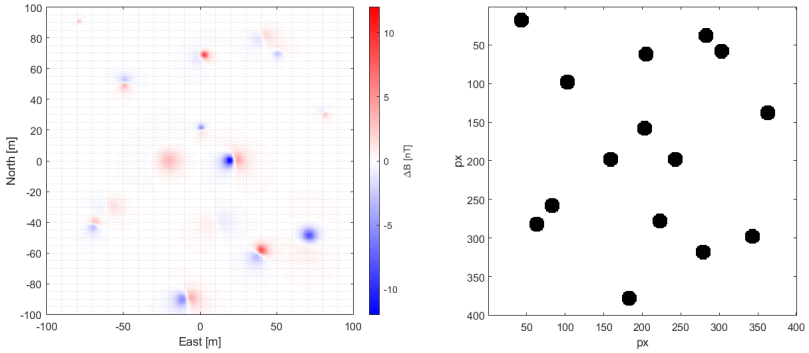

Fig. 1: Example of the simulated TMI data (left) and the labled data (right) of a multi-dipole scenario with 15 anomalies (ground truth)

Subsequently, the simulated samples were transferred into a 400×400 pixel image, depending on the predefined step size in the x- and y-directions and the model domain. Further preparation includes compressing the 2D images to optimize the computational performance of the network. Since the original TMI values are assigned to each pixel, compressing the input information is realized by color coding where a data type transformation from `double` (64 bit) to unsigned integer `uint8` with RGB-channels (each 8 bit) was performed. This leads to the final input feature map.
In semantic segmentation, we are dealing with supervised learning where each pixel is classified as either a background pixel or a pixel of the target class. Thus, labeling the training data appends contextual information and is essential to instruct the model what it actually should learn. This is done by creating a mask with labeled features (magnetic anomalies), which produces the so-called ground truth, for each sample (Fig. 1 right). It contains two channels for a two-class-segmentation, one represents the anomaly and the inverted one the background class. The labels denote the anomaly position by black circles whose centers correlate to the actual dipole coordinates and whose radii correlate to a potential position accuracy. Afterwards, input image and mask are supplied to the learning algorithm which has been implemented in Python. Training and evaluation is performed using the Keras API for Tensorflow.

3 Network Architecture and Model Training

To analyze the generated data, based on the U-Net architecture of Ronneberger et al. (2015), we apply this special deep convolutional neural network (CNN) to geomagnetic data for image segmentation. Our network architecture is presented in Fig. 2, following an encoder-decoder concept by using a large number of multi-channel feature maps denoted by the different boxes, and multiple operations denoted by the box colors and connecting arrows.

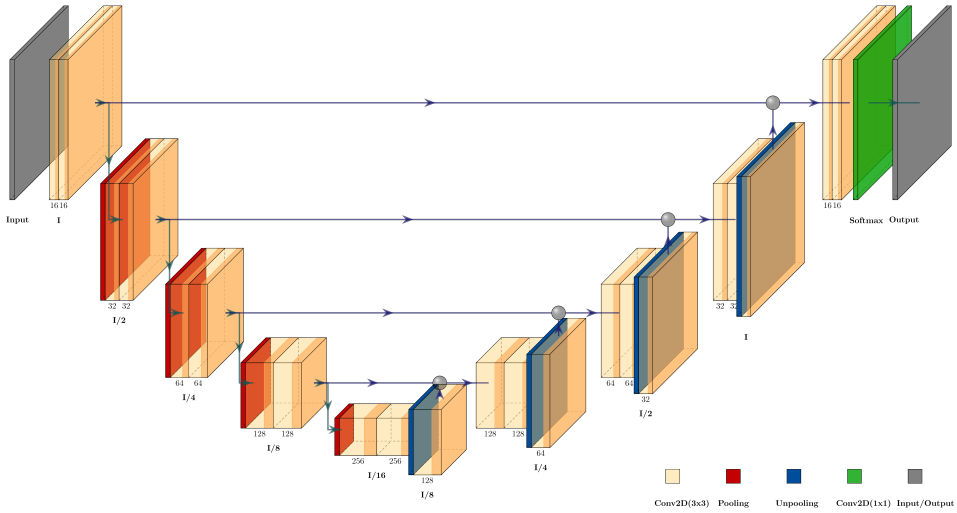

Fig. 2: U-Net architecture for semantic image segmentation

The network learns to segment images end-to-end, where a raw image is supplied to the network and a segmentation map will be returned. This means a classification of each pixel as background or target.
By splitting a 10000-sample synthetic dataset into three parts, the network is trained on 5000 samples and validated on 2000 samples to build a representative model for the chosen scenario. After training, this model is able to predict yet unknown data from the remaining 3000 samples that form the evaluation set. Afterwards, the prediction quality of the resulting model has to be analyzed to fine-tune the training hyperparameters and, if necessary, the network architecture itself. At best, the final segmentation map, i.e. the prediction of the model at the end of the training, should not differ significantly from the ground truth presented before.

4 Evaluation for Exemplary Models

In the following, preliminary results of two model scenarios are discussed. Figs. 4 and 4 each present the model input, i.e., the data and the ground truth (expected output), followed by the segmentation map (predicted output) and a misfit plot between ground truth and segmentation map.
In scenario 1 (Fig. 4), the investigation area contains 19 randomly placed magnetic objects with depths of of 3, 5, 7, or 9 m. The depth value is randomly assigned to an individual object. Temporarily, all sphere radii are kept constant to 0.05 m. The model was trained for clean data and finally evaluated for clean as well as noisy samples. In scenario 2 (Fig 4)

the objects of scenario 1 are assigned randomly generated values from 0 m (earth's surface) to 15 m (subsurface).

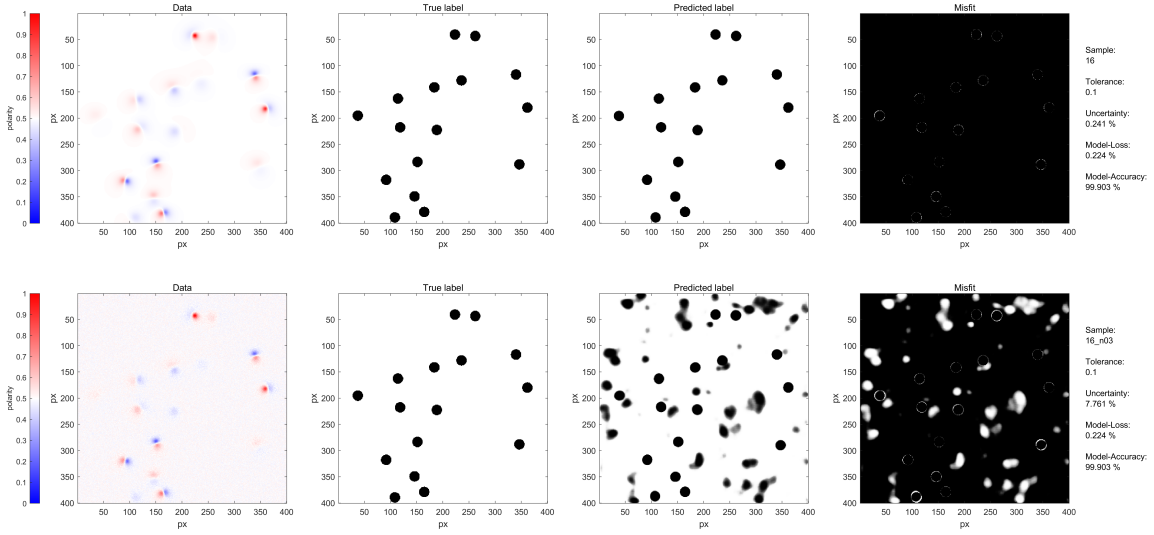

Fig. 3: Modeling results for scenario 1. Top panel: noise-free data sample, bottom panel: noisy data sample. From left to right: Input sample, ground truth, segmentation map, misfit (black represents good fit)

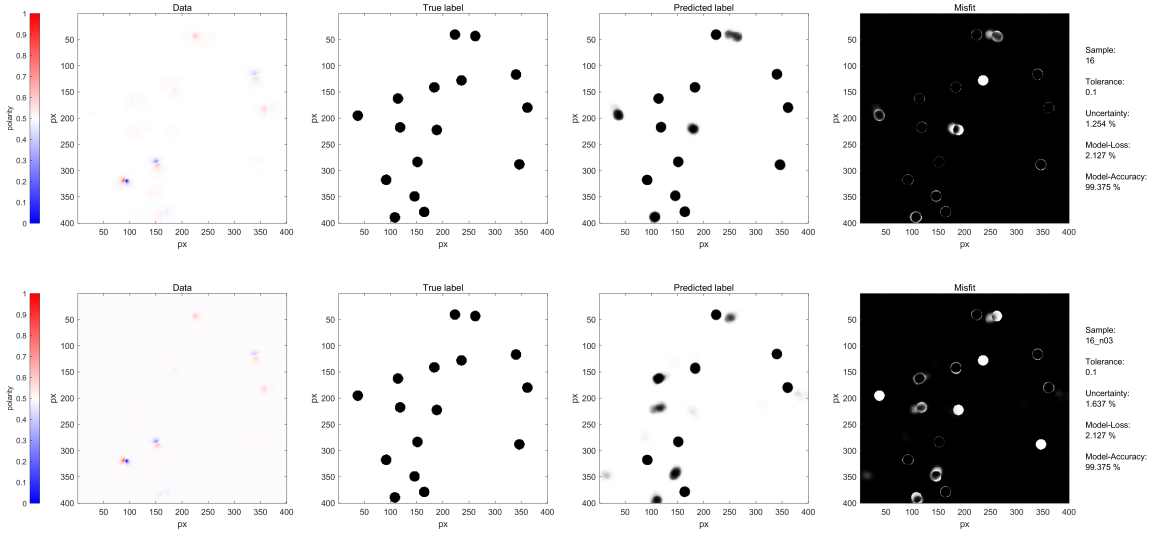

Fig. 4: Modeling results for scenario 2. Top panel: noise-free data sample, bottom panel: noisy data sample. From left to right: Input sample, ground truth, segmentation map, misfit (black represents good fit)

For the training process, several hyperparameters such as the number of data samples, epochs and batch size are defined. Epochs represent the number of training cycles that the learning algorithm will work through using the entire training set. They contain the

so-called mini-batches, which are processed before the models internal parameters are updated. The batch size defines a number of subsamples, used in a single iteration, for which a gradient update is calculated.
An evaluation of the model-generating neural network and the quality of the resulting model itself can be carried out based on several criteria. On the one hand, one could perform a subjective evaluation, e.g., by a direct visual comparison of ground truth and prediction using a misfit plot as in Figs. 4 and 4. On the other hand, one could carry out a quantitative evaluation by assessing model history in terms of loss function and model accuracy, root-mean-square (RMS) analysis of a given number of samples evaluated, or an estimate of prediction uncertainty. The latter may be reached by defining a threshold for the calculated probability of the respective class. For this, we set a tolerance value to 0.1 so that uncertainty corresponds to the percentage of all pixels with probabilities between 0.1 and 0.9. That is, the higher the uncertainty, the less reliable the prediction because the model was not able to accurately predict the anomaly or background class. Thus, just a tendency for the affected pixels is provided. It holds for instance for blurred edges, overlaying noise, or in connection with a displacement between the expected and actual predicted position. However, one have to be careful because, at worst, the network can give an absolute certainty and still makes a wrong prediction.
But these are not the only aspects to be considered. It is also of great importance on which database a model is trained and finally evaluated. In the presented scenarios, it is noticeable that the anomalies of particularly deep-lying objects fall within the signal range of the additive noise floor and thus unwanted artifacts are generated. This significantly reduces the prediction quality (see e.g. the misfit in Fig. 4).

5 Conclusion and Outlook

By focusing on the overlap of magnetic signals in dipole clusters, the U-Net approach allows for a better discrimination of individual anomaly signals, which leads to a more reliable data interpretation. Furthermore, the application of this deep learning approach facilitates the detection of weak anomaly amplitudes in the presence of additive noise. However, it should be taken into account that the model needs to be re-trained with both noisy and clean data in order to cover a wider range of possible scenarios and avoid the generation of artifacts due to an unknown error floor. For this reason, we will extend and combine existing datasets in further investigations. Furthermore, we will evaluate the influence of variable sphere radii making the model assumption more realistic with respect to the maximum achievable prediction accuracy of the model. Additionally, a data transformation, which scales the input in a preprocessing step, shall be analyzed for better recognizability.

References

Blakely, R. J. (1996). *Potential theory in gravity and magnetic applications.* Cambridge: Univ. Press.

Gödickmeier, P. (2020). *Methodische Untersuchungen zur Entwicklung einer hochauflösenden Magnetsensoreinheit für Drohnen.* Masterthesis, Institute for Geopysics and Geoinformatics, TU Bergakademie Freiberg.

Ronneberger, O., Fischer, P., & Brox, T. (2015). U-net: Convolutional networks for biomedical image segmentation. *CoRR, abs/1505.04597.*